

Frequency domain fluorimetry using a mercury vapor lamp

Matthew J. Bohn, Michael A. Lundin and Michael A. Marciniak

Air Force Institute of Technology, Department of Engineering Physics,
2950 Hobson Way, Wright-Patterson AFB, OH USA 45433-776

matthew.bohn@afit.edu

michael.lundin@us.af.mil

michael.marciniak@afit.edu

Abstract. Frequency Domain (FD) fluorimetry, capitalizes on the frequency response function of a fluorophore and offers independence from light scatter and excitation/emission intensity variations in order to extract the sample's fluorescent lifetime. Mercury vapor lamps, a common source of industrial facility lighting, emit radiation that overlaps the UV/blue absorption spectrum of many fluorophores and may be used as an efficient and portable excitation source. The AC power modulation of mercury vapor lamps modulates the lamp's intensity at 120 Hz (in the United States) and higher harmonics. The fluorescent lifetimes for 3 different materials (willemite, uranium doped glass and U_3O_8) are measured with conventional techniques and compared with the FD technique using the power harmonics from a mercury vapor lamp. The mercury lamp measurements agree to within 25% of the conventional methods.

Keywords: frequency domain fluorimetry, phase fluorimetry, remote sensing.

1 INTRODUCTION

Remote detection of minerals has been demonstrated using solar reflectance spectroscopy; however, trace quantities from small nuclear spills [1] is an important problem that is impossible to detect using this method. Uranium quickly oxidizes to form uranyl compounds, UO_2^{2+} , (the +6 oxidation state of uranium) that fluoresce brightly in the green under blue/ultraviolet radiation. The spectral fluorescence can be a good indicator of the presence of uranium. An additional marker is the tell-tale lifetime of this fluorescence, which is extremely long lived ~ 0.6 milliseconds. UV laser induced fluorescence fluorimetry has been previously demonstrated for uranium prospecting [2]. This method measured both the fluorescence spectrum and the fluorescent lifetime in order to identify the uranium minerals; however, the disadvantage is that it requires high power UV radiation on the target when used for remote sensing. This report details a new method of remote sensing long lived UV-active fluorophores by exploiting ambient mercury vapor lamps that occur at the target sight. Mercury vapor lamps are prevalent throughout the world for parking lots and security lighting surrounding facilities and can provide up to 500 W in the UV/blue spectrum. This research effort explores the use of mercury vapor lamps modulated at facility power in order to determine fluorophore's lifetime using Frequency Domain (FD) fluorimetry as a new method of remote sensing UV-active fluorophores such as uranyl compounds. Clear, or uncoated, mercury vapor lamps emit approximately 50% of their optical output (see Fig. 1) in the UV/blue region of the spectrum in emission lines at 365, 405 and 436 nm.

Report Documentation Page

Form Approved
OMB No. 0704-0188

Public reporting burden for the collection of information is estimated to average 1 hour per response, including the time for reviewing instructions, searching existing data sources, gathering and maintaining the data needed, and completing and reviewing the collection of information. Send comments regarding this burden estimate or any other aspect of this collection of information, including suggestions for reducing this burden, to Washington Headquarters Services, Directorate for Information Operations and Reports, 1215 Jefferson Davis Highway, Suite 1204, Arlington VA 22202-4302. Respondents should be aware that notwithstanding any other provision of law, no person shall be subject to a penalty for failing to comply with a collection of information if it does not display a currently valid OMB control number.

1. REPORT DATE DEC 2008		2. REPORT TYPE		3. DATES COVERED 00-00-2008 to 00-00-2008	
4. TITLE AND SUBTITLE Frequency domain fluorimetry using a mercury vapor lamp				5a. CONTRACT NUMBER	
				5b. GRANT NUMBER	
				5c. PROGRAM ELEMENT NUMBER	
6. AUTHOR(S)				5d. PROJECT NUMBER	
				5e. TASK NUMBER	
				5f. WORK UNIT NUMBER	
7. PERFORMING ORGANIZATION NAME(S) AND ADDRESS(ES) Air Force Institute of Technology, Department of Engineering Physics, 2950 Hobson Way, Wright-Patterson AFB, OH, 45433-776				8. PERFORMING ORGANIZATION REPORT NUMBER	
9. SPONSORING/MONITORING AGENCY NAME(S) AND ADDRESS(ES)				10. SPONSOR/MONITOR'S ACRONYM(S)	
				11. SPONSOR/MONITOR'S REPORT NUMBER(S)	
12. DISTRIBUTION/AVAILABILITY STATEMENT Approved for public release; distribution unlimited					
13. SUPPLEMENTARY NOTES					
14. ABSTRACT see report					
15. SUBJECT TERMS					
16. SECURITY CLASSIFICATION OF:			17. LIMITATION OF ABSTRACT	18. NUMBER OF PAGES	19a. NAME OF RESPONSIBLE PERSON
a. REPORT unclassified	b. ABSTRACT unclassified	c. THIS PAGE unclassified			

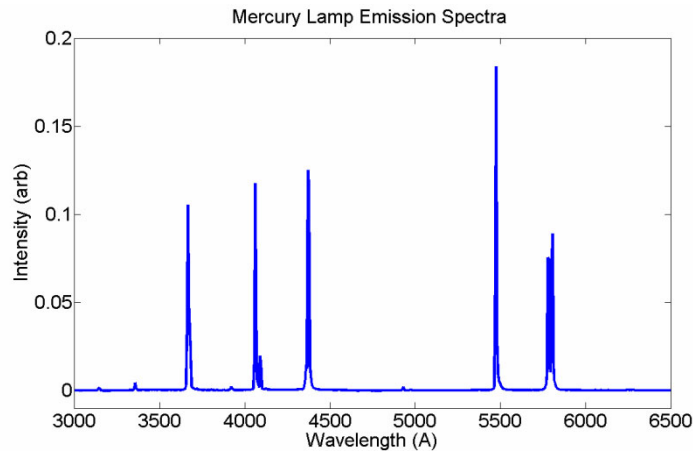


Fig. 1. Mercury vapor lamp (175 Watt) emission spectrum recorded with a 0.5 m monochromator.

For this research effort, fluorophores (willemite, vaseline glass, and yellow cake) were chosen because of their long lifetimes and absorption spectra that matched the emission spectra of mercury vapor lamps. Vaseline glass and yellow cake contain UO_2^{2+} , which absorbs strongly from 390 – 450 nm, has high quantum yields for emission, in the range of 0.4 to 0.8, and a long lifetime, ranging from 0.1 to 0.6 ms [2]. Additionally, the fluorescence emission from these fluorophores occurs at wavelengths (~530 nm) in which the mercury lamp has little output (see Fig. 1). FD fluorimetry can aid in the detection of fluorophores in remote sensing applications since measurements in the frequency domain enable a degree of independence from the problems of light scatter and excitation/emission intensity variations [3].

2 THEORY

The simplest model for the temporal response of a fluorophore is a single exponential decay. By abruptly terminating the excitation source (i.e. using a pulsed UV laser [2]) and then observing the fluorescent intensity as a function of time, the decay can be observed, averaged and stored on a digitizing oscilloscope. The fluorescent lifetime, τ , can be measured by fitting the decaying amplitude to an exponential decay:

$$I(t) = A_0 \exp\left(-\frac{t}{\tau}\right) \quad (1)$$

The experimentalist must insure that the excitation source turns off much more quickly than τ and that the measurement equipment is much faster than τ . Of course the lifetime of the fluorophore will depend on the properties of the host medium due to nonradiative relaxation mechanisms [4]. The single exponential decay modeled above is actually an ensemble average of many fluorophores in the sample. It is assumed in this research effort that the multi-exponential decay times are separated by less than 20 percent such that a single exponential decay is a valid mean value for the fluorophore [4].

FD fluorimetry is a technique that determines the lifetime of the fluorophore by measuring the phase shift and amplitude of the fluorescence when the excitation source is sinusoidally modulated. The excitation modulation will result in an emission delay relative to excitation and can be measured as a phase shift [5]. A sinusoidal excitation source with modulation frequency, ω , will result in a frequency dependent fluorescence of:

$$I(t) \propto m(\omega) \sin(\omega t + \phi(\omega)) , \quad (2)$$

where the phase delay, $\phi(\omega)$, and modulation depth, $m(\omega)$, are determined by the lifetime of the fluorophore and the frequency by:

$$\tan(\phi(\omega)) = \omega\tau \text{ and } m(\omega) = \frac{1}{\sqrt{(1 + \omega^2\tau^2)}}. \quad (3)$$

In traditional FD, the modulation frequency is varied and the phase and modulation amplitude are measured using a lock-in amplifier. Alternatively, the in-phase and quadrature components can be recorded and the lifetime calculation is extracted by least squares analysis of recorded data using the in-phase, N_ω , and quadrature, D_ω , amplitudes of the fluorescent intensity by:

$$N_\omega = \frac{\int_0^\infty I(t) \sin(\omega t) dt}{\int_0^\infty I(t) dt} \text{ and } D_\omega = \frac{\int_0^\infty I(t) \cos(\omega t) dt}{\int_0^\infty I(t) dt}, \quad (4)$$

where the experimental values of $\phi_c(\omega)$ and $m_c(\omega)$ are given by

$$\tan(\phi_c) = \frac{N_\omega}{D_\omega} \text{ and } m_c = (N_\omega^2 + D_\omega^2)^{1/2}. \quad (5)$$

The lifetime can then be calculated such that χ^2 is minimized in

$$\chi^2 = \frac{1}{\nu} \sum_\omega \left(\frac{\phi - \phi_c}{\delta\phi} \right)^2 + \frac{1}{\nu} \sum_\omega \left(\frac{m - m_c}{\delta m} \right)^2, \quad (6)$$

where the values of $\delta\phi$ and δm represent the uncertainty in the measured values, and ν is the number of degrees of freedom.

In the case of the mercury vapor lamp, the modulation frequency is determined by the facility power and higher harmonics and is not controlled in the experiment. All of the frequency components are simultaneously modulated, but since each of the frequency components are linearly independent, the response of each frequency component can be extracted. The lamp's intensity is given by:

$$I_{lamp}(t) \propto \sum_{n=1}^{n_{max}} A_n \sin(2\pi n f_0 t + \phi_n) \quad (7)$$

where f_0 is twice the modulation of facility power ($f_0 = 120$ Hz in the United States). The fundamental modulation is twice the modulation of facility power because the gas discharge rectifies the applied alternating current. One might expect a consistent relationship between the phase of the harmonics, ϕ_n , however, such a relationship could not be experimentally determined. The modulation amplitude, B_n , of the fluorescence can still be used to determine the lifetime after it is normalized by the modulation amplitude of the lamp, A_n , via:

$$I_{fluorescence}(t) \propto \sum_{n=1}^{n_{max}} B_n \sin(2\pi n f_0 t + \theta_n) \quad (8)$$

$$m_n = \frac{1}{\sqrt{(1 + (2\pi n f_0 \tau)^2)}} = \frac{B_n}{A_n}. \quad (9)$$

Since the lamp frequency response is measured using the same experimental equipment as the fluorophore, the response of the entire system is included in the spectral coefficients, A_n . Because the response function of the entire system is removed by taking the ratio B_n/A_n , the systematic error of the FD method is reduced in comparison with a temporal

lifetime measurement. In temporal measurements, the response time of the system is typically minimized to reduce the effect of the system's response on the measurement. The goal of this research effort is not to improve upon previous methods for measuring the lifetime of a fluorophore, but to demonstrate that the power harmonics in a common mercury vapor lamp could be used for remote sensing FD fluorimetry. In this report the test sample of willemite is described in detail because the uranium samples have been presented in a previous publication [6].

3 EXPERIMENTAL

The lifetime of the mineral, willemite, (zinc silicate, $Zn_2SiO_4:Mn$) was measured using the three methods outlined in the introduction. The temporal method will be described first, followed by the traditional FD fluorimetry and finally the FD fluorimetry using a mercury lamp will be described.

3.1 Temporal lifetimes

The equipment for the temporal measurement included a 1 W, 400 nm UV LED (Cree 7090 XLamp) as the excitation source, a Spec 0.5 m monochromator, a C31034 PMT and a digitizing oscilloscope. A UV bandpass filter was used to insure the LED contained no spectral components in the green portion of the spectrum. A spectral scan of the LED revealed that the emission peak occurred at 396 nm. The monochromator wavelength was then moved to 396 nm and the LED was modulated at 250 Hz using a square wave. A 0.5 M Ω resistor terminated the PMT in order to increase the signal to noise ratio, which also increased the system response time, but not to such an extent that the accuracy of the measurement was compromised. The negative edge of the square wave was recorded on the oscilloscope and the single exponential was fit with a decay of 0.08 ms, which is roughly an order of magnitude faster than the fluorescence. This validates the requirement that the system response be much faster than the measured fluorescence. Next the willemite sample was illuminated with the square wave modulated LED and the emission spectrum was recorded. The spectral peak of the willemite emission occurred at 530 nm. The monochromator wavelength was then set to 530 nm and the emissive decay recorded on the oscilloscope (see Fig. 2).

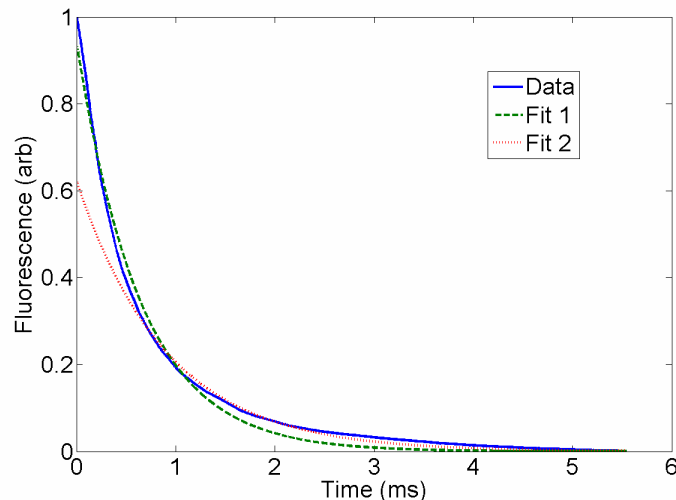


Fig. 2. Temporal lifetime measurement. Fit 1 includes all data ($\tau = 0.64$ ms). Fit 2 removes initial 0.5 ms with exponential fit of 0.86 ms.

When the entire data set is fit with a single exponential, the lifetime was determined to be 0.64 ms. The data appears to contain a multiple exponential decay and using a common practiced technique, the initial 0.5 ms of the decay was removed from the fitting routine, yielding a single exponential lifetime of 0.86 ms. This range of values on the fit indicates the degree of confidence on the fits, which is roughly $\sim 15\%$ of the lifetime value.

3.2 Traditional frequency domain fluorimetry

For the traditional FD technique, the oscilloscope was replaced with a lock-in amplifier. The excitation frequency response function was determined by moving the monochromator wavelength to 396 nm and recording the amplitude from the lock-in amplifier as the HP 33120A function generator frequency was scanned from 1 – 4000 Hz. For the FD technique, the LED was modulated with a sinusoidal signal, in order to avoid multi-frequency excitation. The monochromator wavelength was then repositioned to 530 nm, the peak of the willemite fluorescence, and the magnitude of the fluorescence was measured as a function of frequency from the lock-in amplifier. The ratio of the frequency response, B_n/A_n , is plotted in Fig. 3. The frequency response is fit to equation (9), which yielded a lifetime of 0.51 ± 0.03 ms; where the error is determined from the fit statistics.

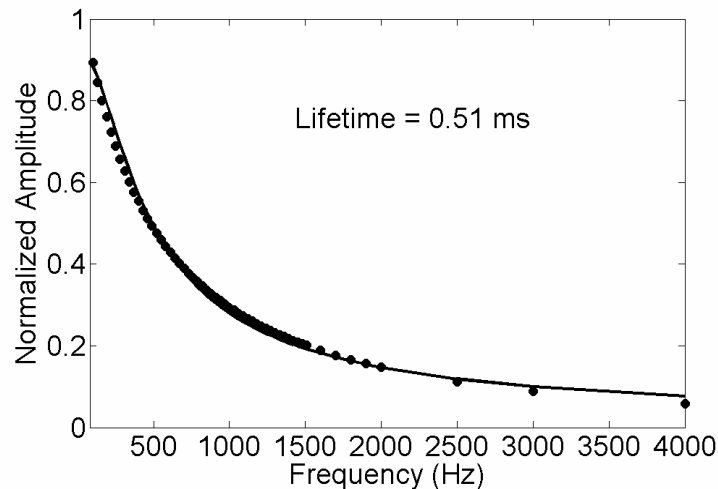


Fig. 3. FD response of willemite using an UV LED as excitation source. Lifetime is 0.51 ms.

3.3 Frequency domain fluorimetry using a mercury vapor lamp

For the mercury vapor lamp excitation, the amplitude of the power harmonics needed to be measured, so the light was detected with a photodiode and the modulation spectrum recorded on a Tektronix RSA3308A RF spectrum analyzer. As can be seen in Fig. 4, the modulation extends beyond 3000 Hz.

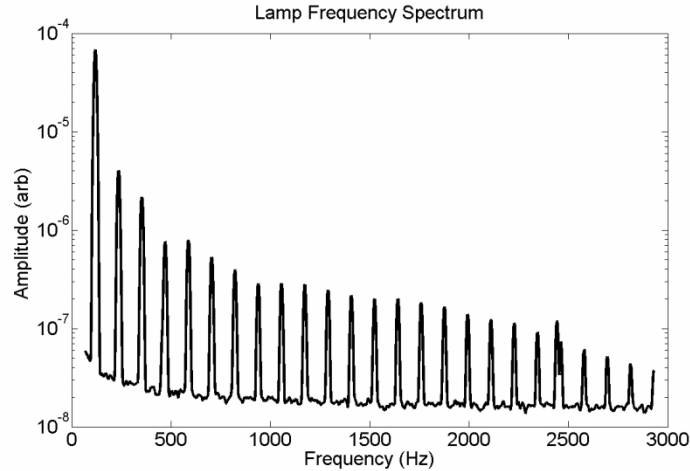


Fig. 4. Power modulation spectrum of mercury vapor lamp measured with an RF spectrum analyzer.

In our experiment, the spectral components were limited to the first 10 harmonics (1200 Hz), due to a reduction in the signal-to-noise at higher frequencies. For the FD method to be successful, the excitation modulation frequency must be constant during the data recording. A closer inspection of the 120 Hz line, see Fig 5, shows a linewidth of 0.052 Hz, which is in excellent agreement with the $\pm 0.05\text{Hz}$ standard published by IEEE and the North American Electric Reliability Council.

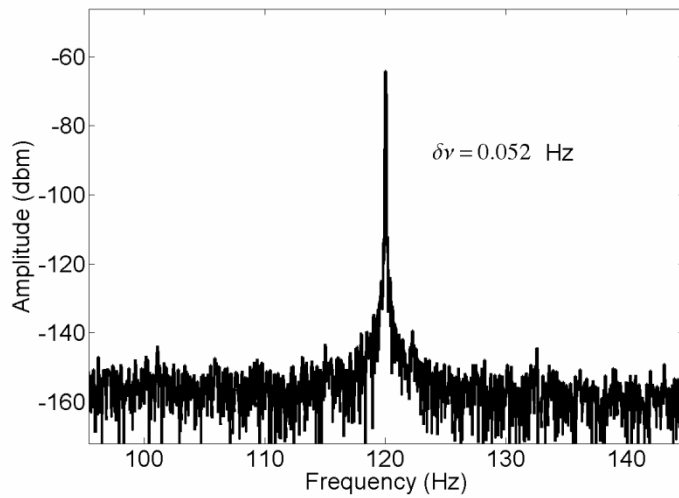


Fig. 5. Modulation spectrum of mercury vapor lamp, zoomed in on 120 Hz line.

In order to correct for the instrument response, the mercury lamp's modulation spectrum was also recorded using the lock-in amplifier. An amplified silicon photodiode signal provided the reference frequency for the lock-in amplifier at 120 Hz. The higher harmonics were sampled using the harmonic function on the lock-in amplifier. Finally, a Chroma green filter centered at 520 nm with a bandwidth 40 nm was positioned in front of the PMT in order to observe the fluorescence from the willemite. The ratio of the response functions is plotted in Fig 6 and the lifetime of willemite using equation 9 was determined to be 0.64 ms from the mercury vapor lamp excitation.

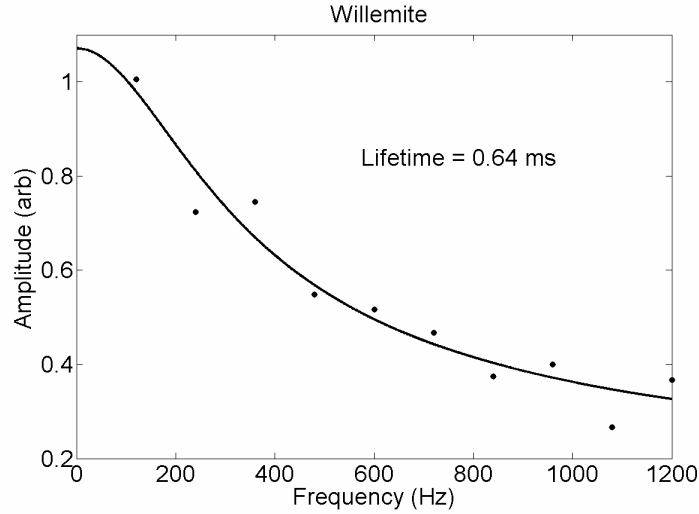


Fig. 6. Frequency response of willemite using a mercury vapor lamp for the excitation source.

3.4 Uranium compounds

Using similar experimental methods, two uranyl, UO_2^{2+} , compounds were also investigated [6]. The first was a sample of UO_2^{2+} doped glass, commonly called vaseline glass, which can be found in antique stores and typically contains less than 2% uranium. The second sample was yellow cake, which is U_3O_8 and is actually a mixture of UO_2 and UO_3 oxides. The same three measurements were made the samples of vaseline glass and yellow cake; namely, a pulsed temporal measurement, FD using an LED and FD using a mercury vapor lamp. Because of the faster lifetime of the uranyl fluorophores, a 50Ω terminator was used on the PMT in order to decrease the system response time. A summary of the results is displayed in Table 1, the error in these values is estimated to be 15% of the lifetime value.

Table 1. Summary of sample lifetime versus detection method.

Sample	Temporal Lifetime (ms)	FD using LED (ms)	FD using Hg lamp (ms)
Willemite	0.64	0.51	0.64
Vaseline Glass	0.27	0.25	0.25
Yellow Cake	0.35	0.32	0.36

4 REMOTE SENSING RANGE CALCULATIONS

The real utility of this technique requires an examination of the geometrical configuration of the source and detector (see Fig. 7) to determine if a usable and reliable signal can be captured at realistic operational distances.

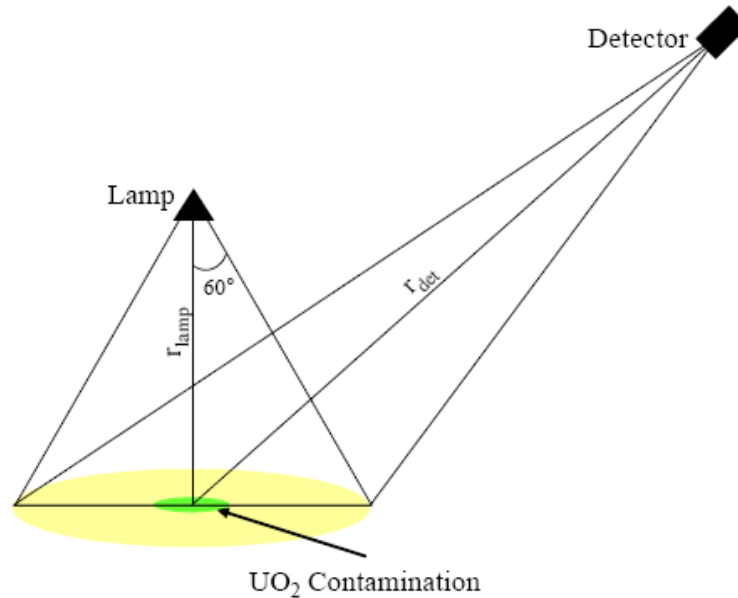


Fig. 7. Detector and source geometry where h is the height of the lamp above the ground and R_{obs} is the target-to-detector range.

There are many unknowns, such as real world concentrations of UO_2^{2+} and atmospheric conditions at observation time. The following describes a conservative approximation of the signal at the detector.

The fundamental equation for radiometry is,

$$L_s = \frac{\partial^2 \Phi_s}{\partial A_s \cos \theta_s \partial \Omega_d} \quad (10)$$

where L_s is the radiance of the source in $\frac{\text{watt}}{\text{m}^2 \text{Sr}}$, Φ_s is the flux of the source in watts, A_s is the area of the source in m^2 , θ_s is the angle between the source-detector ray and the source surface normal ($\cos \theta_s$ provides projected area of the source), and Ω_d is the solid angle subtended by the detector defined as $\Omega_d = \frac{A_d \cos \theta_d}{R^2}$ where A_d is the area of the detector, θ_d is the angle between the source-detector ray and the detector surface normal ($\cos \theta_s$ provides projected area of the detecting surface), and R is the source-to-detector range. The irradiance on a detecting surface in $\frac{\text{watt}}{\text{m}^2}$ is then

$$E_d = \int \frac{L_s \cos \theta_s \cos \theta_d}{R^2} dA_s. \quad (11)$$

In our scenario, the irradiance on the ground due to the lamp is estimated by assuming the lamp is emitting as a point source of uniform intensity into the lower hemisphere and has a reflector collecting the radiation in the upper hemisphere and distributing it uniformly downward into a 60° cone. (According to the engineering bulletin produced by Osram-Sylvania [7], a bulb with a reflector radiates power within a cone of half

angle of 60°.) The ground irradiance is

$$E_{ground}(r, h) = \frac{\Phi_{lamp}}{2\pi} \left[\frac{\cos \theta_d(r, h)}{2(r^2 + h^2)} + \frac{1}{h^2 \cos 60^\circ} \right], \quad (12)$$

where r is the radial distance out from the center point directly below the lamp, h is the height of the lamp and Φ_{lamp} is the total lamp power.

Although the ground is often approximated as Lambertian, we include the more realistic case of increased reflectance as incident angles approach grazing incidence. The assumption of a purely Lambertian surface would increase fluorophore emission and decrease lamp reflection as incident angle, θ_d , increases. Ground reflectance was parameterized using the Schlick approximation for Fresnel reflectance as

$$\rho(r, h) = \rho_{diff} + (1 - \rho_{diff})[1 - \cos \theta_d(r, h)]^5 \quad (13)$$

where hemispherical reflectance near normal incidence for common construction materials such as concrete and asphalt can range $0.1 < \rho_{diff} < 0.35$ in the blue/UV and are consistently ~0.05 higher in the green [2, 3].

By integrating the lamp's spectrum over the wavelengths of interest (see Fig. 1), it can be seen that 50% of the total output is in the blue/UV region ($\eta_{exc} = 0.5$) and approximately 0.5% is in the green region ($\eta_{refl} = 0.005$). While we included an increase in reflectance as incident angles approach grazing, which is normally associated with more specular reflection, we are assuming that the reflected light is perfectly diffused by the ground because this provides a much simpler mathematical model than performing a full bidirectional reflectance distribution function radiosity computation. Realistically, specular reflection does not remain perfect but is scattered into a specular lobe - we have merely broadened this lobe to its full extent. This approach should provide the most conservative estimate since more light is scattered in the direction of the observer from the entire illuminated area than would be if these rays were to be reflected only into their specular direction. With this, the radiances of the reflected lamp in the green and the fluorophore are

$$L_{refl}(r, h) = \frac{[\rho(r, h) + 0.05]\eta_{refl}E_{ground}(r, h)}{\pi} \quad (14)$$

$$L_{fluor}(r, h) = \frac{[1 - \rho(r, h)]\eta_{exc}\eta_{QE}\eta_{ppm}E_{ground}(r, h)}{\pi} \quad (15)$$

respectively, where $0.5 < \eta_{QE} < 0.8$ is the quantum efficiency of the fluorophore [2] and η_{ppm} accounts for the concentrations of the uranium compounds in the ground. While naturally occurring concentrations are <50 ppb in vegetation and 1-10 ppm in soil [8,9], it is expected that accidental releases would yield higher concentrations.

The flux collected by a detecting surface in watts is $\Phi_d = \iint \frac{L_s \cos \theta_s \cos \theta_d}{r^2} dA_s dA_d$.

The fluxes of the reflected lamp in the green and the fluorophore at a collection optic are

$$\Phi_{refl}(h) = \frac{\pi^2 D_{opt}^2 \cos \theta_{obs}}{2R_{obs}^2} \int_0^{r_{max}} r L_{refl}(r, h) dr \quad (16)$$

$$\Phi_{fluor}(h) = \frac{\pi^2 D_{opt}^2 \cos \theta_{obs}}{2R_{obs}^2} \int_0^{r_{max}} r L_{fluor}(r, h) dr \quad (17)$$

respectively, where D_{opt} is the diameter of the optic aperture, θ_{obs} is the observation angle

measured from the surface normal, R_{obs} is the source-to-observer range, and $r_{\text{max}} = \frac{D_{\text{det}} R_{\text{obs}}}{2f / \# D_{\text{opt}}}$ is the maximum radial distance over which the flux is integrated, assuming

the field of view is centered on the point directly below the lamp, where D_{det} is the detector size and $f/\#$ is of the optical system.

Parameters for the Hamamatsu model C4777-01 avalanche photodiode are used in this example since this detector has a flat response over the frequencies of interest (120-1500 Hz). Although detectors are available with a higher spectral response, it is this detector's extremely low noise equivalent power (NEP) of 2-4 $\frac{\text{femtowatt}}{\sqrt{\text{Hz}}}$ that makes it attractive for this

application. Using a noise-equivalent bandwidth, $\Delta f = 0.05 \text{ Hz}$, from the line-width of US power, integration time is $\tau_{\text{int}} = \frac{1}{2\Delta f} = 10 \text{ s}$ and $\text{NEP} \cong 1 \text{ femtowatt}$. The C4777-01 also has

size, $D_{\text{det}} = 3 \text{ mm}$. As a conservative example, for a 400-watt lamp at a height of 9.1 m, $\rho_{\text{diff}} = 0.35$, fluorophore concentration of 10 ppm and quantum efficiency of 50%, an observation distance of 10 km at $\theta_{\text{obs}} = 30^\circ$, and an $f/2$ optical system with a 10-inch optic, the collected fluorophore flux is $> 1 \text{ picowatt}$. This three order-of-magnitude margin above the NEP should account for losses not included here like atmospheric extinction and turbulence, and a signal-to-noise ratio desired to be much greater than one.

The power calculation is applicable if the background signal does not contain fluorescent material with a lifetime similar to the fluorophore of interest. Our experimental results demonstrated the amplitude only FD technique by using only the amplitude modulation of the mercury vapor lamp. If a significant background signal exists, then a more stringent requirement using the fractional background contribution must be met. For a conservative estimate, we assume that the background fluorescent signal is equal to the power reflected from the ground surface. The fractional reflectance contribution, f_B , is defined as the ratio of the lamp's reflected signal to the total signal that is passed through the bandpass filter. A scenario where the fractional contribution is less than one-half the total signal may be desirable for unambiguous extraction of the fluorophore lifetime. This is a more taxing scenario, but also achievable as shown in the Figure 8 examples.

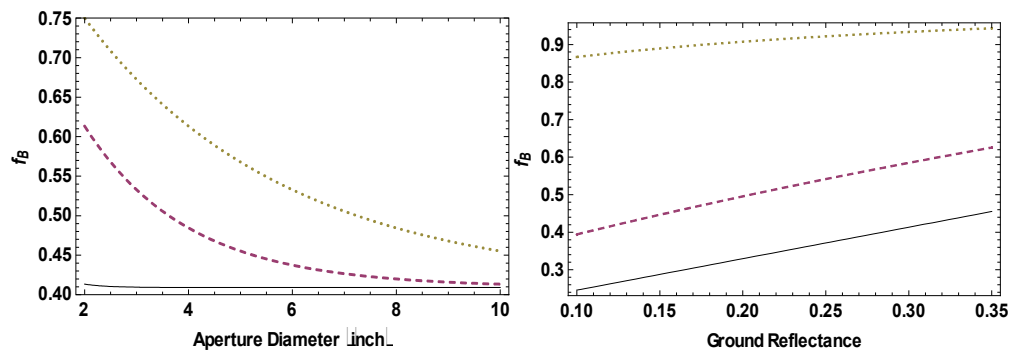


Fig. 8. Fractional contribution, f_B , of the lamp's reflected signal to the total signal. Lamp height is 9.1 m, fluorophore quantum efficiency is 50%, and the optical system is $f/2$ with a 3-mm detector. (a) $\rho_{\text{diff}} = 0.35$, fluorophore concentration is 2%, and observation distances of 1 km (solid line), 5 km (dashed line) and 10 km (dotted line). (b) Observation distance is 10 km, optic aperture diameter is 10 inches, and fluorophore concentration of 2% (solid line), 1% (dashed line) and 0.1% (dotted line).

Here, f_B is independent of lamp flux and θ_{obs} because f_B is a ratio. Figure 8a shows that for a

lamp height of 9.1 m, $\rho_{diff} = 0.35$, fluorophore quantum efficiency of 50%, and an f/2 optical system with 3-mm detector, observation of a fluorophore concentration of 2% meets this requirement with a 2-inch optic at a range of 1 km, a 4-inch optic at 5 km or an 7.5-inch optic at 10 km. Figure 8b shows that for a lamp height of 9.1 m, fluorophore quantum efficiency of 50%, observation distance of 10 km, and an f/2 optical system with a 10-inch optic and 3-mm detector, although observation of a fluorophore concentration of 0.1% never meets this requirement, observation of a fluorophore concentration of 1% meets this requirement for $\rho_{diff} < 0.2$ and of a 2% concentration for $0.1 \leq \rho_{diff} \leq 0.35$.

5 CONCLUSION

This research effort has demonstrated a remote detection method using the multi-frequency excitation of a common mercury lamp via the modulation of facility power at twice the applied AC current and higher harmonics. Although this technique is not as precise as conventional laser and other FD techniques, it enables a novel method of remote sensing without active illumination such as a UV laser. Since the lamp source provides multiple frequency excitation, the detection can be enhanced through parallel, multichannel data collection reducing loiter time over the target area or increasing data collection time [10]. In an application, this method would be employed with more traditional spectroscopic techniques such as emissive spectroscopy of the sample; where the combined information from both spectroscopy and FD would yield a more robust detection. In the future we hope to demonstrate fluorophore imaging using a high speed (at least 2000 frames/second) intensified camera.

References

- [1] National Security Program Office. Formation and Characterization of UO₂F₂ Particles as a Result of UF₆ Hydrolysis. Oak Ridge, TN: National Security Program Office, K/NSP-777, (1998).
- [2] J. P. deNeufville, A. Kasdan, and R. J. L. Chimenti. "Selective detection of uranium by laser-induced fluorescence: a potential remote-sensing technique," *Appl. Opt.* **20**, 1279-1296 (1981). [[doi:10.1364/AO.20.001279](https://doi.org/10.1364/AO.20.001279)]
- [3] P. Harms, J. Sipior, N. Ram, G. Carter, and G. Rao. "Low Cost Phase-Modulation Measurements of Nanosecond Fluorescence Lifetimes Using a Lock-in Amplifier," *Rev. Sci. Instrum.* **70**, 1535-1539 (1999). [[doi:10.1063/1.1149620](https://doi.org/10.1063/1.1149620)]
- [4] J. R. Lakowicz, *Principles of Fluorescence Spectroscopy*, 2nd Edition. (Academic/Plenum Publishers, 1999).
- [5] M. Gaft, R. Renata, and G. Panczer. *Luminescence Spectroscopy of Minerals and Materials* (Springer-Verlag, 2005).
- [6] M. A. Lundin and M. J. Bohn, "Remote Sensing phase fluorimetry using a mercury vapor lamp," *Proc. SPIE*, **6555**, (2007). [[doi: 10.1117/12.718606](https://doi.org/10.1117/12.718606)]
- [7] Sylvania Engineering Bulletin. *SFA-HID-MEREB-069*. 2006.
- [8] D. Earing, Target Signature Analysis Center: Data compilation, Second supplement. Ann Arbor, MI: University of Michigan, 8492-5-B (1967).
- [9] D. Carmer, Target Signature Analysis Center: Data compilation, Seventh supplement Ann Arbor, MI: University of Michigan, 8492-35-B (1969).
- [10] B. A. Feddersen, D. W. Piston, and E. Gratton, "Digital parallel acquisition in frequency domain fluorimetry," *Rev. Sci. Instrum.* **60**, 2929-2936, (1989). [[doi:10.1063/1.1140629](https://doi.org/10.1063/1.1140629)]

Matthew J. Bohn is an assistant professor in the Department of Engineering Physics at the Air Force Institute of Technology. He received his BS degree in physics from the United States Air Force Academy in 1988, a MS in Physics and a PhD in Optical Sciences from the University of New Mexico in 1993 and 1995. Lt Col Bohn conducts research in femtosecond lasers, terahertz spectroscopic imaging and remote sensing. He is a member of SPIE and OSA.

Michael A. Lundin: Michael Lundin received his BS in Physics in 2002 from Midwestern State University and an MS in Applied Physics in 2007 from the Air Force Institute of Technology. He is currently assigned to the Defense Threat Reduction Agency as a staff scientist in the Research and Development Directorate.

Michael Marciniak received his BS degree in mathematics-physics from St. Joseph's College in 1981, his BSEE degree from the University of Missouri-Columbia in 1983, and his MSEE and PhD degrees from the Air Force Institute of Technology (AFIT) in 1987 and 1995, respectively. He is a retired Air Force Lieutenant Colonel and currently an Associate Professor in the Department of Engineering Physics at AFIT with research interests in optical and infrared signatures and opto-electronic material and device physics.